

Article

# Quantitative Analysis of the Factors Influencing the Spatial Distribution of *Benggang* Landforms Based on a Geographical Detector

Kaitao Liao <sup>1,2</sup> , Yuejun Song <sup>2</sup>, Songhua Xie <sup>2</sup>, Yichen Luo <sup>1</sup>, Quan Liu <sup>3</sup> and Hui Lin <sup>1,\*</sup>

<sup>1</sup> College of Geography and Environment, Jiangxi Normal University, Nanchang 330022, China; liaokaitao@jxnu.edu.cn (K.L.); luoyichen@jxnu.edu.cn (Y.L.)

<sup>2</sup> Key Laboratory of Soil Erosion and Prevention, Jiangxi Academy of Water Science and Engineering, Nanchang 330029, China; syj@asch.whigg.ac.cn (Y.S.); kygl2021@jxsl.gov.cn (S.X.)

<sup>3</sup> College of Land Resources and Environment, Jiangxi Agriculture University, Nanchang 330045, China; liuquan@cric.com

\* Correspondence: huilin@cuhk.edu.hk

**Abstract:** As a unique phenomenon of soil erosion in the granite-red-soil hilly area of southern China, *Benggang* has seriously affected agricultural development and regional sustainable development. However, few studies have focused on the driving factors and their interactions with *Benggang* erosion at the regional scale. The primary driving forces of *Benggang* erosion were identified by the factor detector of the geographical detector, and the interaction between factors was determined by the interaction detector of the geographical detector. The 10 conditioning driving factors included terrain, hydrology, vegetation, soil, geomorphology, and land use. *Benggang* erosion in Ganzhou City principally occurred in the granite-red-soil forest hill, characterized by an elevation below 400 m above sea level, slope below 25° of concavity, a distance to the gully less than 500 m, a vegetation coverage of 40–60%, and an average rainfall erosivity of 6400–7000 MJ·mm/(hm<sup>2</sup>·h·a). The key driving factors for *Benggang* erosion were rainfall erosivity, elevation, and land use. Moreover, the interaction of any two factors was stronger than that of a single factor, and the nonlinear enhancement factors had a stronger synergistic effect on erosion. Therefore, the comprehensive influence of many factors must be considered when predicting and preventing *Benggang* erosion.

**Keywords:** *Benggang* erosion; impact factors; geo-detector method; red soil region in South China



**Citation:** Liao, K.; Song, Y.; Xie, S.; Luo, Y.; Liu, Q.; Lin, H. Quantitative Analysis of the Factors Influencing the Spatial Distribution of *Benggang* Landforms Based on a Geographical Detector. *ISPRS Int. J. Geo-Inf.* **2022**, *11*, 337. <https://doi.org/10.3390/ijgi11060337>

Academic Editors: Godwin Yeboah and Wolfgang Kainz

Received: 13 April 2022

Accepted: 2 June 2022

Published: 7 June 2022

**Publisher's Note:** MDPI stays neutral with regard to jurisdictional claims in published maps and institutional affiliations.



**Copyright:** © 2022 by the authors. Licensee MDPI, Basel, Switzerland. This article is an open access article distributed under the terms and conditions of the Creative Commons Attribution (CC BY) license (<https://creativecommons.org/licenses/by/4.0/>).

## 1. Introduction

*Benggang* erosion was first named by the local people in Guangdong Province, China. Then, Zengzaoxuan introduced the term to geomorphology in 1960 [1]. It can be summarized as a kind of collapsed landform formed by the collapse of a soil (stone) body under the combined action of water and gravity [2,3] and is mainly distributed in the red soil areas of Guangdong, Jiangxi, and some other provinces of South China [4–6]. The distribution of *Benggang* erosion is closely related to climate, topography, lithology, and other natural factors [7–9], mainly dispersed in the granite area of tropical and subtropical regions, with obvious zonal, regional, and vertical distribution characteristics [10–12]. The annual average erosion modulus of *Benggang* is approximately 50,000 t km<sup>-2</sup> yr<sup>-1</sup> [13,14]. According to the soil erosion intensity scales established by the Ministry of Water Resources, China (SL190-2007), the erosion intensity is at the most serious intensity level of severe erosion [15]. *Benggang* erosion destroys the topography, produces a large amount of sediment, deposits sediments in rivers, inundates farmland, endangers food security, degrades soil, and threatens ecological security. During the past 60 years, farmland has been the most seriously eroded by *Benggang* erosion. More than 3800 km<sup>2</sup> of farmland has been destroyed, and one-fifth of it cannot be restored [16,17].

A complete typical *Benggang* watershed consists of five geomorphic components: upper catchment, collapsing wall, colluvium deposit (slope water deposit), scour channel,

and alluvial fan (commonly known as sandy land) [4,18]. It is a special type of soil erosion in the red soil region of South China [19,20]. The erosion process has experienced the main stages of the upper gully head, the re-erosion of the middle colluvium cone, the recession of the gully wall, and the formation of the lower alluvial fan [21,22]. Some landforms named badlands in other countries and districts, such as Voco-roca in Northeast Brazil [23,24], Calanchi in Italy [25,26], Lavaka in Madagascar [27,28], and Tabernas in Spain [29,30], are similar to *Benggang* landforms in China (Figure 1).



**Figure 1.** A typical *Benggang*.

In the early phase, researchers focused on the mechanism, monitoring, and prevention of *Benggang* erosion. Approximately 80% of *Benggang* deposits occur in granite weathering crusts [12,31]. Soil water infiltration is the triggering factor of *Benggang* and the precondition for *Benggang* formation [32,33]. Using a 3D laser scanner, unmanned aerial vehicles, and other technical monitoring tools for *Benggang* erosion [10,34,35], the maximum retreat rate was reported to be 11.7 m/a [19]. Then, some scholars studied the influences of lithology, soil, topography, rainfall, temperature, and other natural factors on the distribution of *Benggang* landforms. High temperatures and rainy climates in subtropical humid areas lead to deep weathering crusts and provide erosion power that promote *Benggang* development [22,36,37]. *Benggang* erosion is mainly distributed in the granite parent material area [38,39]; has a vertical spatial distribution in the 100–500 m elevation of hilly areas [40,41], with large and heavy rain; and is also related to human activities [42,43]. Exploring the key driving factors and distribution characteristics of *Benggang* erosion is helpful to providing a theoretical basis for the prevention and control of *Benggang* erosion. Some scholars use the logistic model [44], gray relational grade analysis [45], and the niche-fitness [46] model to study the relative importance of *Benggang* erosion factors.

*Benggang* is a complex landform formed by the combined action of multiple factors. There were about  $2.4 \times 10^5$  *Benggang* in the red soil region of southern China. Ganzhou City is a typical *Benggang* erosion area, with  $3.2 \times 10^4$  *Benggang* widely distributed. Its ecological safety, food security, and people's life safety have been threatened by the *Benggang* erosion. However, there are few studies on *Benggang* erosion in Ganzhou City, and its multi-factor interactions are still unclear [47].

With the development of remote sensing technology and geographical information system (GIS) technology, regional data acquisition and overlay analysis have become possible [48,49]. Moreover, the geographical detector model can effectively identify the relationship between multiple factors, such as independent or interactive interactions, enhanced or weakened interactions, and linear or nonlinear interactions [50,51]. The geographical detector was first used to assess the relative importance of different factors controlling or contributing to disease and then expanded to other fields (such as land use, geology, and environment). Therefore, the study of the multi-factor interaction relationship of *Benggang* erosion has become possible.

The objectives of this study are to explore the distribution characteristics of *Benggang* in southern China by using GIS and the geographical detector and to analyze the main driving factors and their interaction in terms of the *Benggang* erosion. This study would explore the multi-factor interaction relationship of *Benggang* erosion and provide a scientific basis for *Benggang* erosion harness in southern China, where *Benggang* erosion is widely distributed and considered as one of the main types of eroded land.

## 2. Materials and Methods

### 2.1. Study Area

Ganzhou City is in South China, within a longitude of 113°54' E to 116°38' E and a latitude of 24°29' N to 27°09' N (Figure 2), occupying 39,400 square kilometers, and it is the largest prefectural city of Jiangxi Province [52]. The amount of *Benggang* erosion in Jiangxi Province is the second largest in China, while 67.02% of the locations are in Ganzhou City, mainly located in *Ganxian* County, *Xin'guo* County, and *Yudu* County. It was the earliest management area of water and soil erosion in China.

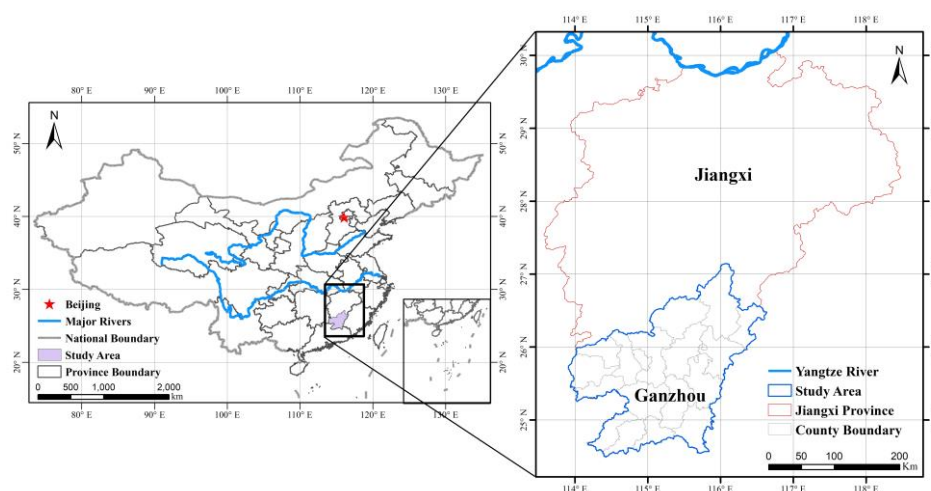


Figure 2. Geographical map of the study area.

The study area is on the southern edge of the middle subtropical zone and belongs to the typical subtropical humid monsoon climate zone, with an annual average rainfall of 1587 mm. The annual average temperature is approximately 18.9 °C, and the accumulated temperature (>10 °C) is between 5000 °C and 6000 °C [53]. The average elevation in the digital elevation model (DEM) is 200 m, and the main morphology type is mountainous and hilly. The main soil type is red soil developed from granite. The regional climate, lithology, and topographical conditions provide favorable internal and external conditions for the development of *Benggang* erosion.

### 2.2. Data Sources

The *Benggang* erosion data, including the number, area, and location information, were from the investigations of *Benggang* erosion in South China from 2004 to 2005 by the

Ministry of Water Resources of China (Yangtze River Water Conservancy Commission) and the *Benggang* erosion survey in Jiangxi Province in 2015 by the Ministry of Water Resources of Jiangxi Province.

The Advanced Spaceborne Thermal Emission and Reflection Radiometer Global Digital Elevation Model (ASTER GDEM 30) and land use and land cover (30 m) data (Geospatial Data Cloud, Computer Network Information Centre of the Chinese Academy of Sciences, <http://www.gscloud.cn>, accessed on 31 May 2020), the 1:2.5 million geological maps (China Geological Survey, <https://www.cgs.gov.cn/>, accessed on 15 June 2020), the daily rainfall data for the study area and adjacent stations (total of 26) from 1960 to 2016 (China National Meteorological Information Center, <http://data.cma.cn/en>, accessed on 26 June 2020), the 1:1 million soil-type maps (Resource and Environment Science and Data Center, <https://www.resdc.cn/>, accessed on 8 July 2020), and Landsat data (Aerospace Information Research Institute, Chinese Academy of Sciences, <http://ids.ceode.ac.cn/>, accessed on 18 July 2020) were used.

The Ganzhou *Benggang* erosion database was established based on the *Benggang* erosion survey in Jiangxi Province in 2015 by the Ministry of Water Resources of Jiangxi Province by ArcMap 10.2, and the survey assessed the area, average depth, and width of the gully and the longitude and latitude of the geographical coordinates. The spatial query, spatial statistics, and overlay analysis function of ArcMap 10.2 was used to analyze the spatial distribution characteristics of *Benggang* erosion under the conditions of 10 factors. The geographical detector method was used to analyze the influence degree of different factors on the distribution of *Benggang* erosion and explore the interaction between various factors.

### 2.3. Geographical Detector Method

Geographical detector is a statistical method that can detect spatial differences and reveal the driving factors behind them [54]. The basic idea of this method is to assume that the study area is divided into several regions; if the sum of variance of these regions is less than the total variance of these regions, there are spatial differences. The  $q$ -statistic of the geographical detector can measure the spatial difference and detect the interaction between explanatory factors and analysis variables. When an independent variable has an important influence on a dependent variable, the spatial distributions of the independent variable and the dependent variable are similar. The geographical detector can analyze both numerical data and qualitative data, and it can detect an interaction between the two factors.

The geographical detector has four detectors (factor, interaction, ecological, and risk detectors), of which factor and interaction detectors were most effective in the quantitative assessment of ecological environmental impact factors [50,55]. Therefore, we used the factor and interaction detectors in this paper.

The factor detector was used to detect the spatial differentiation of the *Benggang* erosion and the influence of the factor on the spatial differentiation of the *Benggang* erosion. The value was measured by the  $q$  value.

$$q = 1 - \frac{\sum_{h=1}^L N_h \sigma_h^2}{N \sigma^2}$$

where  $h = 1, \dots, L$  is the layer of independent variable  $X$  and  $N_h$  and  $N$  are the number of sample units in layer  $h$  and the total region  $Y$ , respectively. Moreover,  $\sigma_h^2$  and  $\sigma^2$  are the variance in the  $h$  layer and the variance in the region. The  $q$  value lies in  $[0, 1]$ . The larger the value of  $q$ , the stronger the explanatory power of this factor on the differentiation of *Benggang* erosion, and vice versa. In this study,  $Y$  is *Benggang* erosion and  $X$  is the influencing factor.

The interaction detector was used to evaluate whether the two factors could enhance or weaken the impact on the spatial distribution of the *Benggang* or whether these factors were independent of each other. First, calculate the  $q$  values  $q(X_1)$  and  $q(X_2)$  of factors  $X_1$  and  $X_2$ , respectively. Then, calculate the  $q$  value  $q(X_1 \cap X_2)$  of the interaction between

factors  $X_1$  and  $X_2$  according to the relationship between  $q(X_1)$ ,  $q(X_2)$ , and  $q(X_1 \cap X_2)$  to determine their related interaction type. The classification of related interaction types is shown in Table 1.

**Table 1.** Abstract example of types of interaction between two covariates.

Description	Interaction
$q(X_1 \cap X_2) < \text{Min}(q(X_1), q(X_2))$	Weaken, nonlinear
$\text{Min}(q(X_1), q(X_2)) < q(X_1 \cap X_2) < \text{Max}(q(X_1), q(X_2))$	Weaken, single factor nonlinear
$q(X_1 \cap X_2) > \text{Max}(q(X_1), q(X_2))$	Enhanced, double factors
$q(X_1 \cap X_2) = q(X_1) + q(X_2)$	Independent
$q(X_1 \cap X_2) > q(X_1) + q(X_2)$	Enhanced, nonlinear

#### 2.4. Processing of Influencing Factors

Many factors and the interaction between them affect the development of *Benggang* erosion. Research [7,40,42,56] has shown that the development of *Benggang* erosion is limited by elevation, affected by slope gradient and slope type, and has a certain slope aspect selectivity. Soil and geology are important internal factors affecting *Benggang* erosion, and vegetation can inhibit *Benggang* erosion because it has a direct protective effect on the soil. The hydraulic force is the external factor affecting the development of *Benggang* erosion, and frequent and high-intensity rainstorms produce strong rainfall erosivity, which promotes the development of *Benggang* erosion. Human activities are one of the most important factors affecting *Benggang* erosion. According to the actual situation of Ganzhou City, considering the representativeness of factors and the availability of data, and combined with the research results of predecessors, 10 factors, i.e., elevation, slope, aspect, slope type, lithology, soil type, rainfall erosivity, distance to river, vegetation coverage, and land use type, were selected. These factors needed to be graded before they were used in geographical detector. ArcMap 10.2 was used to process and classify the 10 factors. Detailed rules for classification were as follows:

##### (1) Elevation

The DEM (m) was divided into 8 stratifications, <100, 100–200, 200–300, 300–400, 400–500, 500–600, 600–700, and >700 (Figure 3a), which were defined as levels 1–8, respectively.

##### (2) Slope

The slope was calculated by the DEM. The slope ( $^\circ$ ) was divided into 5 stratifications, <5, 5–15, 15–25, 25–35, and >35 (Figure 3b), according to the “General rules for comprehensive control planning of soil and water conservation, China,” [45] which were defined as levels 1–5, respectively.

##### (3) Aspect

Aspect was calculated by the DEM. Aspect was divided into 8 stratifications: north (337.5–360 $^\circ$  and 0–22.5 $^\circ$ ), northeast (22.5–67.5 $^\circ$ ), east (67.5–112.5 $^\circ$ ), southeast (112.5–157.5 $^\circ$ ), south (157.5–202.5 $^\circ$ ), southwest (202.5–247.5 $^\circ$ ), west (247.5–292.5 $^\circ$ ), and northwest (292.5–337.5 $^\circ$ ) (Figure 3c). They were defined as levels 1–8, respectively. The sunny slopes were the southwest, south, southeast, and east slopes and the shady slopes were the northeast, north, northwest, and west slopes.

##### (4) Slope type

Slope type was calculated by the DEM. Slope type was divided into 2 stratifications, convex slope (curvature > 0) and concave slope (curvature < 0) (Figure 3d), which were defined as levels 1–2, respectively.

##### (5) Soil type

The main soil types in the study area are red soils, yellow soils, paddy soils, calcareous soils, fluvo-aquic soils, purple soils, and meadow soils (Figure 3e), which were defined as levels 1–7, respectively.

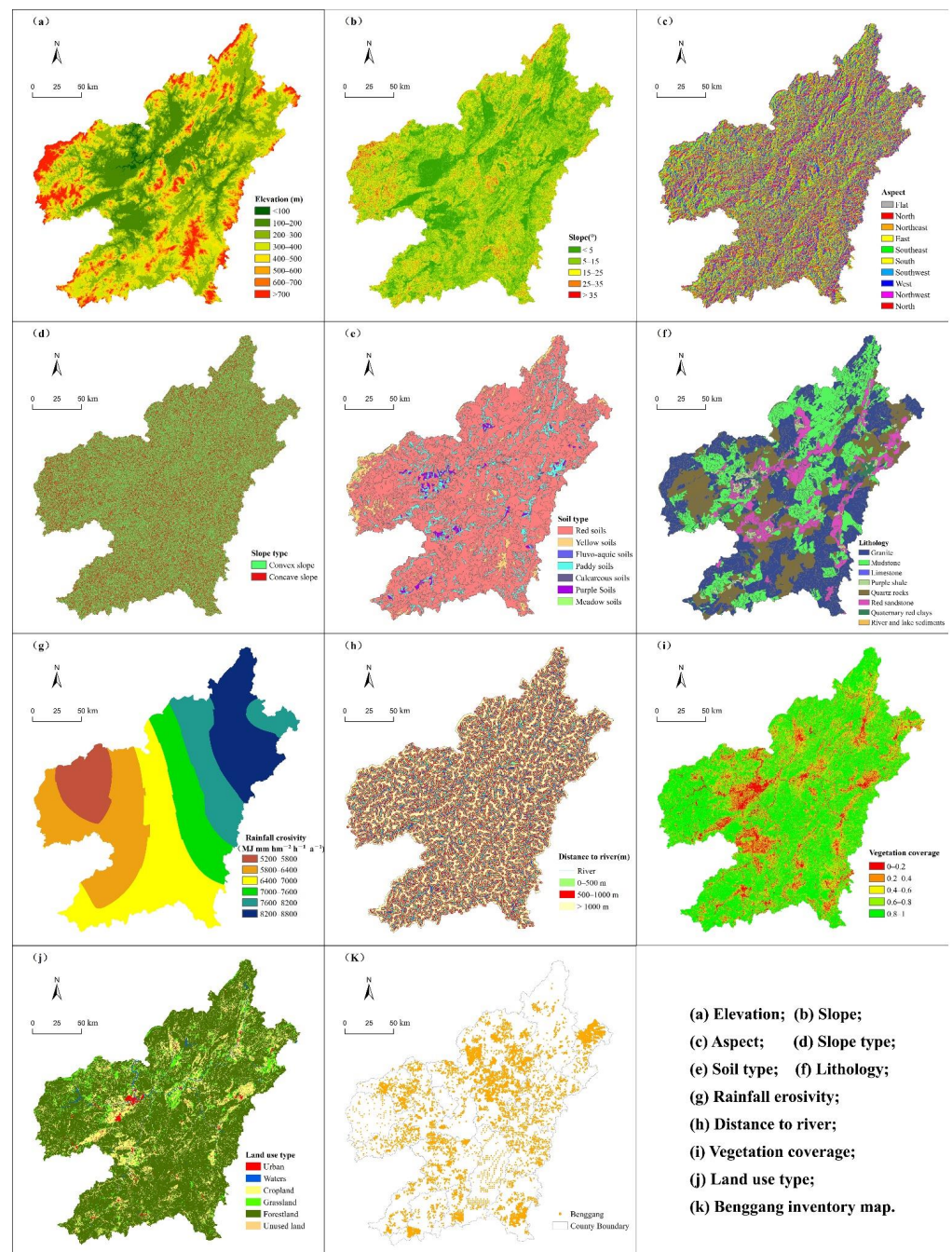


**Figure 3.** Influence factor layers of *Benggang*. (a) elevation; (b) slope; (c) aspect; (d) slope type; (e) soil type; (f) lithology; (g) rainfall erosivity; (h) distance to river; (i) vegetation coverage; (j) land use type; (k) *Benggang* inventory map.

### (6) Lithology

The main lithologies in the study area are granite, mudstone, red sandstone, quartz rocks, purple shale, Quaternary red clays, limestone, and river and lake sediments (Figure 3f), which were defined as levels 1–8, respectively.

### (7) Rainfall erosivity

The daily rainfall data of 26 stations in Ganzhou City and its surrounding counties were downloaded from the national meteorological data sharing network and calculated by the rainfall erosivity method of Wenbo et al. [57,58]. The rainfall erosivity was divided into

6 stratifications: 5200–5800, 5800–6400, 6400–7000, 7000–7600, 7600–8200, and 8200–8800 ( $\text{MJ mm hm}^{-2} \text{ h}^{-1} \text{ a}^{-1}$ ) (Figure 3g). They were defined as levels 1–6, respectively.

(8) Distance to river

The distance (m) to the river was divided into 3 stratifications, <500, 500–1000, and >1000 (Figure 3h), which were defined as levels 1–3, respectively.

(9) Vegetation coverage

The vegetation coverage was calculated by pixel dichotomy [59–61] using the Landsat image of Ganzhou City in 2015 and divided into 5 stratifications, 0–20, 20–40, 40–60, 60–80, and 80–100 (Figure 3i), which were defined as levels 1–5, respectively.

(10) Land use type

The primary land use types in the study area included forestland, cropland, grassland, urban land, water, and unused land (Figure 3j), which were defined as levels 1–6, respectively.

The spatial distribution of *Benggang* erosion is shown in Figure 3k. The *Benggang* point layer intersected with the distribution layers of the 10 influencing factors and the attributes of each *Benggang* point were obtained; these points contained the attributes of the 10 factors. After these operations, the data were analyzed in the geographical detector.

### 3. Results

#### 3.1. Distribution Characteristics of *Benggang* Erosion in Ganzhou City

The distribution characteristics of *Benggang* erosion in Ganzhou were obtained by the overlay analysis function of ArcMap 10.2 (Figure 4). As shown in Table 2, *Longnan* County, *Ganxian* District, and *Yudu* County are among the top three in terms of the number of *Benggang*, with a total of 12516, accounting for 33.86% of the total number. Among them, *Longnan* County has the largest number, with 4354, accounting for 13.48% of the total number. *Zhanggong* District has the fewest number, with 42. Through the analysis of the *Benggang* erosion area, *Ganxian* District was found to have the largest area of *Benggang* erosion, of 38.61  $\text{km}^2$ , accounting for 30.03% of the total area, followed by *Yudu* County and *Xingguo* County, and these three counties account for 39.56% of the total area. The *Benggang* erosion area of the remaining counties is less than 8%. From the perspective of the population density of counties, the top three counties are *Nankang* District, *Ganxian* District, and *Xingguo* County, which have 9231 *Benggang*, accounting for 28.04% of the total number of *Benggang*, and the area is 54.96  $\text{km}^2$ , accounting for 42.75% of the total area of *Benggang* erosion. The population density may contribute to the development of *Benggang* erosion. Based on the density of *Benggang* erosion, the biggest is 2.64/ $\text{km}^2$ , in *Longnan* County, and the smallest is 0.09/ $\text{km}^2$ , in *Zhanggong* District. According to the spatial distribution of the number of *Benggang* erosion occurrences (Figure 1), the *Benggang* erosion areas are mainly distributed in the northern part of Ganzhou City, where *Ganxian* County, *Xingguo* County, and *Yudu* County are the main areas. The distribution is lower in the eastern and western parts of Ganzhou City.

#### 3.2. Distribution Characteristics of *Benggang* Erosion Influencing Factors

The distribution characteristics of *Benggang* erosion influencing factors were obtained by spatial query and overlay analysis function of ArcMap 10.2. As shown in Figure 5a, the number of *Benggang* erosion occurrences first increased then decreased with the increase in the elevation, reaching a maximum at 200–300 m (36.28%), and few events occurred above 600 m (2.04%) and below 100 m (0.23%). The range 100–200 m had the largest area of *Benggang* erosion, and then it declined with elevation. *Benggang* erosion was mainly distributed at 100–400 m (85.76% of the number and 88.97% of the area), which was related to the thickest weathering crust of granite, which is widely distributed in this area.

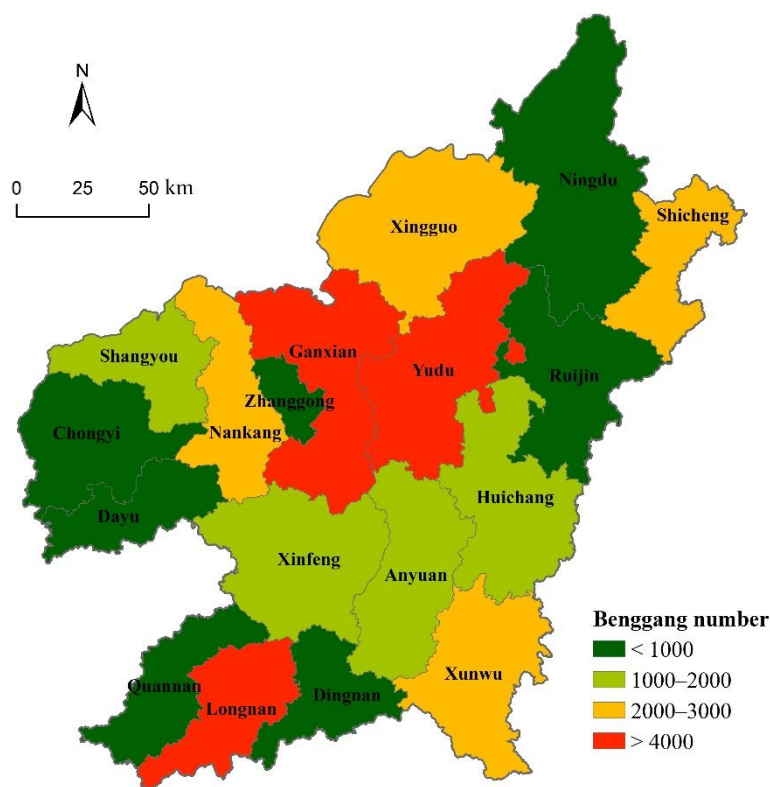


Figure 4. Distribution map of *Benggang* in Ganzhou City.

Table 2. Statistics of *Benggang* in different counties (cities and districts) of Ganzhou City.

District	Number	Area (km <sup>2</sup> )	Population Density (Person/km <sup>2</sup> )	<i>Benggang</i> Density (Unit/km <sup>2</sup> )	District	Number	Area (km <sup>2</sup> )	Population Density (Person/km <sup>2</sup> )	<i>Benggang</i> Density (Unit/km <sup>2</sup> )
Anyuan	1252	4.70	169.57	0.53	Quannan	742	0.82	129.00	0.48
Chongyi	396	0.59	98.27	0.18	Ruijing	948	1.54	287.49	0.39
Dayu	540	0.50	135.69	0.40	Shangyou	1897	1.23	210.19	1.23
Dingnan	787	3.73	168.15	0.60	Shicheng	2468	9.61	210.75	1.57
Ganxian	4136	38.61	218.01	1.38	Xinfeng	1839	10.69	267.78	0.64
Huichang	1386	3.13	194.37	0.51	Xingguo	2933	12.62	263.36	0.91
Longnan	4354	9.83	204.09	2.64	Xunwu	2162	6.28	142.99	0.92
Nankang	2162	5.32	489.24	1.17	Yudu	4026	17.77	383.46	1.39
Ningdu	853	1.43	209.63	0.21	Zhanggong	42	0.17	1939.02	0.09

As shown in Figure 5b, the number of *Benggang* erosion occurrences decreased with increasing slope. Half of these values were at 5–15° (49.3%), 97.90% were concentrated in 0–25°, and few occurred at slopes higher than 35° (0.22%).

As shown in Figure 5c, there was not a big difference in the number of *Benggang* erosion occurrences among the aspects (except flat). The southwest aspect had the highest number (13.47%), and the west aspect had the lowest (11.51%). *Benggang* erosion was slightly more abundant on sunny slopes (south, southwest, west, and northwest) than those on shady slopes (north, northwest, east, and northeast).

As shown in Figure 5d, the percentage of the *Benggang* area and the number on the concave slope were larger than those on the convex slope, both over 60%.



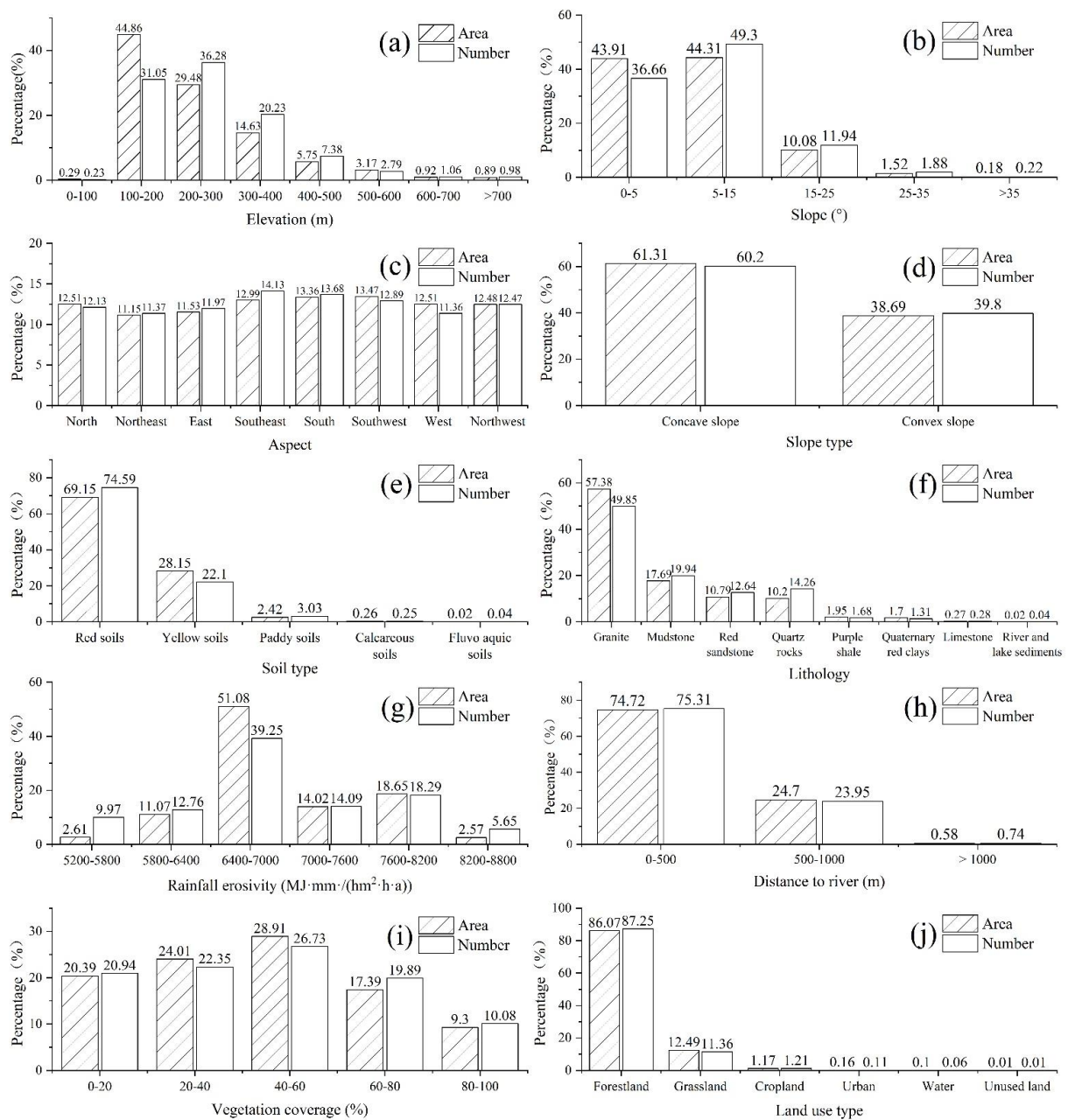


**Figure 5.** The number and area of *Benggang* under each influence factor. (a) elevation; (b) slope; (c) aspect; (d) slope type; (e) soil type; (f) lithology; (g) rainfall erosivity; (h) distance to river; (i) vegetation coverage; (j) land use type.

As shown in Figure 5e, *Benggang* erosion was mainly distributed in the red soils, with 74.19% of the erosion occurring in 69.15% of the area. The number and area of *Benggang* erosion in yellow soils were the second highest, accounting for 22.10% and 28.15%, respectively. Other types of soil accounted for less than 3%.

As shown in Figure 5f, granite was the most susceptible original material soil to *Benggang* erosion and more than half of the *Benggang* erosion occurred in this type. Approximately one-fifth of the *Benggang* erosion occurred in mudstone. Red sandstone and quartz rocks rank third and fourth, respectively.

As shown in Figure 5g, *Benggang* erosion was mainly distributed in the area with rainfall erosivity of 5800–8200 MJ·mm/(hm<sup>2</sup>·h·a), accounting for more than 84.39%. There were obvious differences in the number of *Benggang* erosion occurrences distributed in

regions with different rainfall erosivity levels. The largest number of *Benggang* erosion occurrences was in the region with a rainfall erosivity of 6400–700 MJ·mm/(hm<sup>2</sup>·h·a), accounting for 39.25% of the total.

As shown in Figure 5h, three-quarters of *Benggang* erosion occurred within 500 m of the river, and the number and area of *Benggang* erosion decreased with increasing distance from the river.

As shown in Figure 5i, the number of *Benggang* erosion occurrences first increased and then decreased with fractional vegetation cover (FVC). The number of *Benggang* erosion occurrence areas was mainly distributed in the FVC range of 40–60% (26.73%), followed by 20–40% (22.35%), and the fewest *Benggang* erosion occurrence areas were distributed in the range of 80–100% (9.30%).

As shown in Figure 5j, among the land use types, *Benggang* erosion was dominant in forestland (87.25%), less in grassland (11.36%), and lowest in the other land use types.

### 3.3. *Benggang* Factor Influence Analysis

The factor was used to assess each factor's relative importance. The *Benggang* erosion area was taken as variable *y*, and 10 factors, such as elevation, slope direction, and soil type, were used as the *x* variables. The *q* value of the 10 factors on *Benggang* erosion was obtained by a factor detector, and the *q* value indicated the influence of each factor on *Benggang*. The value of *q* is between 0 and 1, and a larger value means a stronger influence.

As shown in Table 3, the *q* value was in the order of rainfall erosivity > elevation > land use > slope > lithology > vegetation coverage > distance to river > soil type = aspect > slope type. The contributions of rainfall erosivity and elevation were the largest, meaning that the occurrence of *Benggang* erosion was mainly affected by rainfall and elevation.

**Table 3.** Statistical table of *q* value of 10 factors.

Impact Factor	Elevation	Slope Type	Slope	Aspect	Lithology	Soil Type	Distance to River	Rainfall Erosivity	Vegetation Coverage	Land Use Type
<i>q</i> value	0.0111	0.0000	0.0031	0.0003	0.0014	0.0003	0.0005	0.0113	0.0009	0.0035

### 3.4. *Benggang* Factor Interaction Analysis

The interaction detector was used to analyze the interaction relationship of the 10 factors. The 10 factors were made up 55 factor pairs (Table 4). Comparing Tables 3 and 4, the interaction of any two factors was greater than the sum of the *q* values of the two factors and the interaction of any two factors was stronger than that of a single factor, which indicates that the nonlinear enhancement factor had a strong synergistic effect. The interaction effects of the two factors ranked in the top four, from large to small, were elevation and rainfall erosivity, elevation and distance to the river, elevation and land use, and rainfall erosivity and land use. An analysis of the comprehensive interaction between a single factor and the other 9 factors showed that the strongest was rainfall erosivity (0.2025), followed by elevation (0.197), land use (0.1159), and distance to the river (0.0763). The results showed that rainfall, elevation, and human activities were the three most important factors affecting *Benggang* erosion. *Benggang* erosion was affected by the interaction of multiple factors, which should be considered comprehensively in the process of restoration.

**Table 4.** Interaction of 10 impact factors of *Benggang* erosion.

Impact Factor	X1	X2	X3	X4	X5	X6	X7	X8	X9	X10
X1	0.0111									
X2	0.0113	0.0000								
X3	0.0170	0.0031 *	0.0031							

Table 4. Cont.

Impact Factor	X1	X2	X3	X4	X5	X6	X7	X8	X9	X10
X4	0.0143	0.0004	0.0039	0.0003						
X5	0.0330	0.0040	0.0147	0.0074	0.0035					
X6	0.0159	0.0015	0.0059	0.0028	0.0076	0.0014				
X7	0.0131	0.0004 *	0.0041	0.0011	0.0048	0.0017 *	0.0003			
X8	0.0226	0.0011	0.0053	0.0081	0.0096	0.0031	0.0073	0.0005		
X9	0.0455	0.0114	0.0185	0.0121	0.0214	0.0145	0.0123	0.0126	0.0113	
X10	0.0132	0.0011	0.0048	0.0033	0.0099	0.0030	0.0015	0.0061	0.0144	0.0009

X1, X2, X3, X4, X5, X6, X7, X8, X9, and X10 refer to elevation, slope type, slope, aspect, lithology, soil type, distance to river, rainfall erosivity, vegetation coverage, and land use type, respectively. "\*" means that the driving factors x and y have double synergism; for those without "\*", it means that the driving factors x and y have nonlinear synergism.

## 4. Discussion

### 4.1. Impact Factor Contribution Analysis

The regional distribution characteristics of *Benggang* erosion are formed under the combined action of the internal and external factors. The internal factors provide basic material conditions for the *Benggang* erosion. The topography, lithology, and soil are the mainly internal factors.

The distribution characteristics of *Benggang* erosion at different elevation are basically consistent with those of Ganzhou City. The area of 100–300 m in Ganzhou City is the largest, as well as has the largest number of *Benggang* erosion occurrences. *Benggang* erosion is mainly distributed at elevation below 500 m because the weathering effect is strong and the weathering materials are easily preserved at this elevation, which provides a material source for *Benggang* erosion [9,42]. Moreover, vegetation is seriously destroyed by frequent human activities, and without the protection of vegetation, the loose and deep weathering crust is prone to *Benggang* erosion. Most of the areas of Ganzhou City with an elevation of less than 100 m are river valleys, and the terrain is flat, which is not suitable for the development of *Benggang* erosion.

The *Benggang* erosion distribution is concentrated on slopes 5–15°. However, the percentage of this area is the largest in Ganzhou. Additionally, the thickness of the weathering crust is large and there are frequent destructive activities by humans in this area. Therefore, *Benggang* erosion is serious in this area.

*Benggang* erosion on the sunny slope is greater than that on the shady slope. The total solar radiation is greater on the sunny slope, the rainfall erosivity is larger, and due to the large thermal variation and frequent alternation of dry and wet conditions, the shear strength of the soil easily decreases on sunny slopes [62]. Therefore, *Benggang* erosion is more serious on sunny slopes.

Red soils are the main soil type in Ganzhou, and red soils in South China have plate, acid, thin, sticky, and eroded characteristics, especially the red soil parent material layer formed by granite weathering, which has poor anti-erodibility and is prone to *Benggang* erosion [63,64].

*Benggang* erosion is mainly distributed on the granite parent material [33]. In the warm and humid subtropical monsoon climate, the weathering is strong and deep and a loose weathering crust is easily form, which provides the necessary material source for *Benggang* erosion [16]. Meanwhile, there are many joints and fissures in the weathering crust of granite, and the soft structural plane in the weathering crust soil would expand and become increasingly larger under the influence of gravity, rainfall, and other factors. The red sandstone has less *Benggang* erosion because of its strong weathering resistance and thin weathering layer [11].

The external factors provide strength for *Benggang* erosion. The rainfall erosivity, vegetation coverage, and human actives are the main external factors. The rainfall erosivity of Ganzhou City is between 5200 and 8800 MJ·mm/(hm<sup>2</sup>·h·a) and increases from the south-

west to the northeast. The area of rainfall erosivity grade of 6400–7000 MJ·mm/(hm<sup>2</sup>·h·a) is the largest, and it is concentrated in *Ganxian* District, *Yudu* County, and *Longnan* city. The number of *Benggang* erosion areas in these three counties is greater than 4000 and is most serious in Ganzhou City.

Vegetation protects the soil surface from severe erosion by heavy rainfall runoff. It is generally considered that *Benggang* erosion rarely occurs in high-vegetation-coverage areas, though field investigations show that many areas with good vegetation coverage conditions still develop *Benggang*. It may be that the vegetation makes many weathering materials accumulate in situ, which creates conditions for *Benggang*, or the vegetation grew later. The forest in Jiangxi Province has experienced serious damage in the last century. To restore the ecosystem, the government implemented the aerial seeding afforestation ecological project in 1965, and the vegetation restoration effect is remarkable [65]. This may be one of the reasons for the good vegetation coverage in the *Benggang* erosion area.

The forestland area of Ganzhou City accounts for 77% of the total area of Ganzhou City. Most *Benggang* erosion occurs in the *Pinus massoniana* forest area, with a poor ability to intercept rainfall runoff, and less occurs in the coniferous and broad-leaved mixed forest area. Once the vegetation cover disappears, the humus soil on the surface quickly washes away by rain or develops into shallow gullies. When it erodes to the clastic layer below, it easily develops into *Benggang* erosion.

Human activities play an important role in inducing and promoting the development of *Benggang* erosion. In modern times, the irrational development of land resources, predatory mining, improper site selection for reservoirs, improper reclamation of infrastructure, and improper soil collection have accelerated the development of *Benggang* erosion. According to the distribution and occurrence history of *Benggang* erosion, *Benggang* erosion is mostly distributed in low mountains and hills on the edge of the basin (valley) with dense villages, concentrated populations, and convenient transportation but rarely in remote mountain areas with closed traffic and few people. Obviously, this pattern is related to unreasonable human activities. According to the investigation, there have been many instances of deforestation in Ganzhou's history, and deforestation has destroyed the original vegetation, resulting in many bare surfaces, increased runoff, deepened gully cutting, and increased numbers and areas of *Benggang* erosion.

#### 4.2. Multifactor Interaction Analysis

Some scholars have considered *Benggang* erosion as a type of water erosion [21,33], while some scholars think it should belong to the category of gravity erosion [41]. More scholars believe both gravity erosion and water erosion affect *Benggang* erosion and both are indispensable [2,7,42]. Thus, water and gravity are the forces of *Benggang* erosion.

The formation of *Benggang* erosion is influenced by many natural and man-made factors and is a complex system. The results of the factor detector show that rainfall, elevation, and land use are the main factors affecting *Benggang* erosion. Natural rainfall is the main source of soil moisture in *Benggang* erosion [66].

Ganzhou City is in the subtropical monsoon climate area. The average annual rainfall in Ganzhou City is approximately 1587 mm [52]. The rainfall is mostly concentrated in spring and summer, accounting for approximately 70% of the annual rainfall. Heavy rain and rainstorms mainly occur from April to September [67]. In the summer of 1961, the daily rainfall exceeded 200 mm. Abundant rainfall and frequent and high-intensity rainstorm events easily produced strong rainfall erosivity, washed the topsoil, destroyed the soil structure, reduced the soil stability, and provided external power for *Benggang* erosion [68].

Previous studies have shown that the formation of *Benggang* erosion is closely related to the deep and loose weathering crust and this crust is the material basis and internal cause of *Benggang* erosion [41]. The area of Ganzhou City with an elevation of 100–500 m accounts for 80.5% of the total area, where the weathering crust is widely distributed, and the relative elevation difference in topography also provides favorable conditions for gravity erosion of the collapsed granite [45]. Granite is widely distributed in this area.

In the warm, humid, and hot conditions, a deep weathering crust is formed by strong biochemical action, which can generally reach 10–50 m. The weathering crust has a loose structure and strong permeability. During precipitation, the soil moisture easily reaches saturation. Under the action of surface runoff and gravity, the soil easily develops to form *Benggang* erosion.

The area with an elevation of 100–500 in Ganzhou City is also the area with the most intense human activities [69]. Furthermore, the formation of a weathering crust is related to human activities. Unreasonable human activities have destroyed the original vegetation of the mountains, increased the exposed area, intensified runoff, and deepened erosion ditches, increasing the area and number of *Benggang* erosion.

There are many factors that lead to the development of *Benggang* erosion, and the roles of each factor and their relationship are complex [9,56]. The interaction of multiple factors is stronger than that of a single factor. The distribution of the granite weathering crust and human activities is related to elevation. The weathering crust is the internal factor and rain is the external factor affecting *Benggang* erosion. The interaction of these factors is the strongest. The impact factors of *Benggang* erosion in Ganzhou have location-specific characteristics, and targeted prevention and control measures should be taken in the process of prevention and control of *Benggang* erosion.

## 5. Conclusions

Using the spatial distribution of *Benggang* erosion factors extracted from ArcMap, this paper analyzed the influencing factors of *Benggang* distribution in Ganzhou using the geographical detector by considering the geographical strata of the 10 factors. Factors related to terrain, soil, geology, climate, vegetation, and human active were chosen for analysis. By analyzing the  $q$  statistics of the individual factors and how the interaction between factors enhances the results, the factors that are related to *Benggang* erosion in Ganzhou were identified and analyzed. The results showed that the most responsible conditioning factors are rainfall erosivity, elevation, and land use.

Specifically, the conditions appropriate for *Benggang* erosion are an average annual rainfall erosivity of 6400–7000 MJ mm ( $\text{hm}^2 \cdot \text{h} \cdot \text{a}$ ), an elevation of 100–400 m, and an FVC of 40–60%. The areas with high susceptibility to *Benggang* erosion are generally located in a slope below  $25^\circ$  of concave degree, are at a distance from the river of less than 500 m, have concentrated granite weathering crust, and have forestland with red soils. Meanwhile, the factor detector indicated that there are spatial differences in *Benggang* erosion and the top three factors are rainfall erosivity, elevation, and land use. Overall, the interaction detector proved that the distribution of *Benggang* erosion is the result of the interaction of multiple factors. The interaction of any two factors is stronger than that of a single factor, and the nonlinear enhancement factors have the strongest synergistic effect on erosion. The strongest interaction factor pair is rainfall and elevation. The geographical detector can be used in the driving factor analysis of *Benggang* erosion.

The methodological framework of this study exhibits a reasonably satisfactory method for exploring the multi-factor interaction relationship of *Benggang* erosion in Ganzhou, Jiangxi Province, and provides a theoretical basis for the prevention and control of *Benggang* erosion. Meanwhile, it could be implemented in other similar regions with *Benggang* erosion of southern China. Furthermore, the resolution of condition factors should be considered in future works, especially when erosional analysis is performed at regional scales.

**Author Contributions:** This paper was written with contributions of all authors, as follows: conceptualization, Kaitao Liao and Yuejun Song; methodology, Quan Liu and Yuejun Song; formal analysis, Kaitao Liao and Quan Liu; data curation, Kaitao Liao; investigation, Yuejun Song; writing—original draft preparation, Kaitao Liao; writing—review and editing, Hui Lin and Songhua Xie; visualization, Kaitao Liao and Yichen Luo. All authors have read and agreed to the published version of the manuscript.

**Funding:** This research was supported by the National Natural Science Foundation of China (No. 41967011,41867012), the Natural Science Foundation of Jiangxi Province, China (No. 20181BAB203024), and the Water Conservancy Science and Technology Project of Jiangxi Province, China (No. 202124ZDKT25, 202123YBKT16).

**Data Availability Statement:** Not applicable.

**Conflicts of Interest:** The authors declare no conflict of interest.

## References

- Zhang, W.L.; Yuan, Z.J.; Li, D.Q.; Zheng, M.G.; Liao, Y.S.; Cai, Q.Q.; Huang, Y.H.; Cai, C.F.; Niu, D.K.; Wang, Z.G. Discussion of the “Benggang” Concept and Its English Translation. *Sci. Soil Water Conserv.* **2020**, *18*, 136–143.
- Liu, X.L. Benggang Erosion Landform and Research Progress in a Global Perspective. *Prog. Geogr.* **2018**, *37*, 342–351.
- Cai, L.P.; Liu, M.X.; Hou, X.L.; Wu, P.F.; Ma, X.Q. Comparison of Plant Diversity among Different Governance Models in Collapsing Gully Erosion Area of Changting County. *J. Fujian Agric. For. Univ. Nat. Sci. Ed.* **2012**, *41*, 524–528.
- Liu, X.L.; Zhang, D.L. Grain-Size Properties and Morphologic Patterns of Channelized Flows in a Benggang Catchment of Southern China. *Z. Für Geomorphol.* **2018**, *61*, 303–314. [[CrossRef](#)]
- Li, C.; Kong, L.; Shu, R.; An, R.; Zhang, X. Disintegration Characteristics in Granite Residual Soil and Their Relationship with the Collapsing Gully in South China. *Open Geosci.* **2020**, *12*, 1116–1126. [[CrossRef](#)]
- Huang, B.F.; Qiu, M.; Lin, J.S.; Chen, J.; Jiang, F.; Wang, M.K.; Ge, H.L.; Huang, Y.H. Correlation between Shear Strength and Soil Physicochemical Properties of Different Weathering Profiles of the Non-Eroded and Collapsing Gully Soils in Southern China. *J. Soils Sediments* **2019**, *19*, 3832–3846. [[CrossRef](#)]
- Xu, J.X. Benggang Erosion: The Influencing Factors. *Catena* **1996**, *27*, 249–263. [[CrossRef](#)]
- Zhang, P.; Zha, X. The Research Progress on Collapsed Gully Erosion. *Res. Soil Water Conserv.* **2007**, *14*, 170–172.
- Liao, Y.S.; Zheng, M.G.; Li, D.Q.; Wu, X.L.; Liang, C.; Nie, X.D.; Huang, B.; Xie, Z.Y.; Yuan, Z.J.; Tang, C.Y. Relationship of Benggang Number, Area, and Hypsometric Integral Values at Different Landform Developmental Stages. *Land Degrad. Dev.* **2020**, *31*, 2319–2328. [[CrossRef](#)]
- Liao, K.T.; Song, Y.J.; Xie, S.H.; Zheng, H.J. Monitoring of Benggang Erosion Based on UAV Photogrammetry Technology. In *IOP Conference Series: Earth and Environmental Science*; IOP Publishing: Bristol, UK, 2019; Volume 330, p. 052003.
- Deng, Y.S.; Cai, C.F.; Xia, D.; Ding, S.W.; Chen, J.Z.; Wang, T.W. Soil Atterberg Limits of Different Weathering Profiles of the Collapsing Gullies in the Hilly Granitic Region of Southern China. *Solid Earth* **2017**, *8*, 499–513. [[CrossRef](#)]
- Liu, X.L.; Tang, C.; Zhang, D.L. Simulated Runoff Processes on Colluvial Deposits of Liantanggang Benggang and Their Water Distributions. *Trans. Chin. Soc. Agric. Eng.* **2015**, *31*, 179–185.
- Ji, X.; Huang, Y.H.; Lin, J.S.; Jiang, F.S.; Yu, M.M.; Li, S.X. Estimation of erosion amount in collapsed gully based on CA-Markov model and ANUDEM interpolation. *Trans. Chin. Soc. Agric. Eng.* **2018**, *34*, 128–136.
- Dong, X.; Ding, S.W.; Li, L.; Deng, Y.S.; Wang, Q.X.; Wang, S.L.; Cai, C.F. Effects of Collapsing Gully Erosion on Soil Qualities of Farm Fields in the Hilly Granitic Region of South China. *J. Integr. Agric.* **2016**, *15*, 2873–2885. [[CrossRef](#)]
- Zhong, B.L.; Peng, S.Y.; Zhang, Q.; Ma, H.; Cao, S.X. Using an Ecological Economics Approach to Support the Restoration of Collapsing Gullies in Southern China. *Land Use Policy* **2013**, *32*, 119–124. [[CrossRef](#)]
- Deng, Y.S.; Duan, X.Q.; Ding, S.W.; Cai, C.F.; Chen, J.Z. Suction Stress Characteristics in Granite Red Soils and Their Relationship with the Collapsing Gully in South China. *Catena* **2018**, *171*, 505–522. [[CrossRef](#)]
- Long, L.; Ding, S.W.; Cai, C.F.; Xia, D.; Liao, X.W. Damage of collapse erosion to farmland in granite red soil hilly area and its control. *Soil Water Conserv. China* **2013**, *12*, 24–26.
- Zhang, D.L.; Liu, X.L. Evolution and Phases Division of Collapsed Gully Erosion Landform. *J. Subtrop. Resour. Environ.* **2011**, *6*, 23–28.
- Liu, H.; Qian, F.; Ding, W.; Gómez, J.A. Using 3D Scanner to Study Gully Evolution and Its Hydrological Analysis in the Deep Weathering of Southern China. *Catena* **2019**, *183*, 104218. [[CrossRef](#)]
- Deng, Y.S.; Cai, C.F.; Xia, D.; Ding, S.W.; Chen, J.Z. Fractal Features of Soil Particle Size Distribution under Different Land-Use Patterns in the Alluvial Fans of Collapsing Gullies in the Hilly Granitic Region of Southern China. *PLoS ONE* **2017**, *12*, e0173555. [[CrossRef](#)]
- Jiang, F.S.; Huang, Y.H.; Lin, J.S.; Lin, X.; Zhao, G.; Zhang, Y.; Xie, X.F.; Fu, H. The Dynamic Characteristics of Soil Detachment of Slumping Deposit by Surface Runoff in Benggang. *J. Soil Water Conserv.* **2013**, *27*, 86–89.
- Tao, Y.; Zou, Z.Q.; Guo, L.; He, Y.B.; Lin, L.R.; Lin, H.; Chen, J.Z. Linking Soil Macropores, Subsurface Flow and Its Hydrodynamic Characteristics to the Development of Benggang Erosion. *J. Hydrol.* **2020**, *586*, 124829. [[CrossRef](#)]
- De Bacellar, L.A.; Netto, A.C.; Lacerda, W.A. Controlling Factors of Gullying in the Maracujá Catchment, Southeastern Brazil. *Earth Surf. Process. Landf. J. Br. Geomorphol. Res. Group* **2005**, *30*, 1369–1385. [[CrossRef](#)]
- De Menezes Rodrigues, K.; Correia, M.E.F.; de Resende, A.S.; de Lima Camilo, F.; Campelo, E.F.C.; Franco, A.A.; Dechen, S.C.F. Soil Fauna along the Process of Ecological Succession in Gullies Revegetated in the Municipality of Pinheiral-RJ/Fauna Do Solo Ao Longo Do Processo de Sucessao Ecologica Em Vocoroca Revegetada No Municipio de Pinheiral-RJ. *Cienc. Florest.* **2016**, *26*, 355–365. [[CrossRef](#)]

25. Bosino, A.; Omran, A.; Maerker, M. Identification, Characterisation and Analysis of the Oltrepo Pavese Calanchi in the Northern Apennines (Italy). *Geomorphology* **2019**, *340*, 53–66. [[CrossRef](#)]
26. Neugirg, F.; Stark, M.; Kaiser, A.; Vlacilova, M.; Della Seta, M.; Vergari, F.; Schmidt, J.; Becht, M.; Haas, F. Erosion Processes in Calanchi in the Upper Orcia Valley, Southern Tuscany, Italy Based on Multitemporal High-Resolution Terrestrial LiDAR and UAV Surveys. *Geomorphology* **2016**, *269*, 8–22. [[CrossRef](#)]
27. Cox, R.; Bierman, P.; Jungers, M.C.; Rakotondrazafy, A.M. Erosion Rates and Sediment Sources in Madagascar Inferred from <sup>10</sup>Be Analysis of Lavaka, Slope, and River Sediment. *J. Geol.* **2009**, *117*, 363–376. [[CrossRef](#)]
28. Voarintsoa, N.R.G.; Cox, R.; Razanatsheho, M.O.M.; Rakotondrazafy, A.F.M. Relation between Bedrock Geology, Topography and Lavaka Distribution in Madagascar. *S. Afr. J. Geol.* **2012**, *115*, 225–250. [[CrossRef](#)]
29. Rodríguez-Caballero, E.; Cantón, Y.; Jetten, V. Biological Soil Crust Effects Must Be Included to Accurately Model Infiltration and Erosion in Drylands: An Example from Tabernas Badlands. *Geomorphology* **2015**, *241*, 331–342. [[CrossRef](#)]
30. Casali, J.; López, J.J.; Giráldez, J.V. Ephemeral Gully Erosion in Southern Navarra (Spain). *Catena* **1999**, *36*, 65–84. [[CrossRef](#)]
31. Ji, X.; Thompson, A.; Lin, J.S.; Jiang, F.S.; Li, S.X.; Yu, M.M.; Huang, Y.H. Simulating and Assessing the Evolution of Collapsing Gullies Based on Cellular Automata-Markov and Landscape Pattern Metrics: A Case Study in Southern China. *J. Soils Sediments* **2019**, *19*, 3044–3055. [[CrossRef](#)]
32. Tao, Y.; He, Y.; Duan, X.; Zou, Z.; Lin, L.; Chen, J. Preferential Flows and Soil Moistures on a Benggang Slope: Determined by the Water and Temperature Co-Monitoring. *J. Hydrol.* **2017**, *553*, 678–690. [[CrossRef](#)]
33. Duan, X.Q.; Ni, C.; Chen, J.; Chen, J.Z. Study on the Preferential Flow of Red Soil Erosion in Granite slope collapse with High Frequency Monitoring of Water Content. *J. Soil Water Conserv.* **2016**, *30*, 82–88.
34. Shen, S.; Zhang, T.; Zhao, Y.; Wang, Z.; Qian, F. Automatic Benggang Recognition Based on Latent Semantic Fusion of Upr Dome and Dsm Features. *ISPRS Ann. Photogramm. Remote Sens. Spat. Inf. Sci.* **2020**, *5*, 331–338. [[CrossRef](#)]
35. Li, Z.J.; Zhong, L.T.; Huang, Y.H.; Ge, H.L.; Zhu, Y.; Jiang, F.S.; Li, X.F.; Zhang, Y.; Lin, J.S. Monitoring technology for collapse erosion based on the nap of the object photograph of UAV. *Trans. Chin. Soc. Agric. Eng.* **2021**, *37*, 151–159.
36. Wang, Y.H.; Xie, X.D.; Wang, C.Y. Formation Mechanism of Calamities Due to Benggang Processes of Weathered Granitic Rocks. *J. Mt. Sci.* **2000**, *18*, 496–501.
37. Lin, J.L.; Huang, Y.H. Review of Study on Formation Mechanism of Slope Disintegration Erosion and Its Problems. *Res. Soil Water Conserv.* **2010**, *17*, 41–44.
38. Jiang, F.S.; Huang, Y.H.; Lin, J.S.; Zhao, G.; Ge, H.L.; Lin, J.L. Effects of Slope Gradient and Rainfall Intensity on Particle Size Composition of Erosion Sediment from Colluvial Deposits of Benggang. *Acta Pedol. Sin.* **2014**, *51*, 974–982.
39. Zhang, Y.Y. Eroding Soil types and Their Management Counter measures of Granite Regions in Guangdong Province, China. *J. Mt. Sci.* **2009**, *27*, 49–53.
40. Zhang, Y.; Zhao, D.F.; Lin, J.S.; Jiang, L.; Huang, B.F.; Jiang, F.S.; Wang, M.K.; Ge, H.L.; Huang, Y.H. Impacts of Collapsing Gullies on the Dynamics of Soil Organic Carbon in the Red Soil Hilly Region of Southeast China. *Catena* **2020**, *190*, 104547. [[CrossRef](#)]
41. Chen, X.A.; Yang, J.; Xiao, S.S.; Song, Y.J.; Zheng, H.J.; Shen, L. Distribution Characteristics and Causes of Collapse Erosion. *J. Mt. Science* **2013**, *31*, 716–722. [[CrossRef](#)]
42. Liao, Y.S.; Yuan, Z.J.; Zheng, M.; Li, D.Q.; Nie, X.D.; Wu, X.L.; Huang, B.; Xie, Z.Y.; Tang, C.Y. The Spatial Distribution of Benggang and the Factors That Influence It. *Land Degrad. Dev.* **2019**, *30*, 2323–2335. [[CrossRef](#)]
43. Li, S.X.; Gui, H.Z.; Ding, S.W. Features of Special layout of Hill Collapse in South China. *J. Huazhong Agric. Univ.* **2013**, *32*, 83–86.
44. Li, C.M.; Xu, G.L.; Lu, Y. Key Influencing Factors and Susceptibility of Collapse Gully in Southeast Guangxi, China. *J. Yangtze River Sci. Res. Inst.* **2020**, *37*, 131–136.
45. Liao, K.T.; Liu, Y.; Liu, Q.; Song, Y.J.; Huang, H.S. Distribution Characteristics and Driving Factors of Benggang Erosion in Ganzhou City. *Res. Soil Water Conserv.* **2021**, *28*, 126–130. [[CrossRef](#)]
46. Xiang, J.; Huang, Y.; Lin, J.; Jiang, F.; Chen, J. Sensitivity Assessment Method of Collapsed Gully Occurrence in Granite Region of South China Based on Niche-Fitness. *J. China Agric. Univ.* **2017**, *22*, 159–168.
47. Qiu, J.A.; Liu, X.L. Status and Comprehensive Analysis of Benggang Research in China Based on Knowledge Maps. *Sci. Soil Water Conserv.* **2017**, *15*, 139–148.
48. Korchenko, O.; Pohrebennyk, V.; Kreta, D.; Klymenko, V.; Anpilova, Y. GIS and Remote Sensing as Important Tools for Assessment of Environmental Pollution. *Int. Multidiscip. Sci. GeoConference SGEM* **2019**, *19*, 297–304.
49. Xu, F.L.; Tao, S.; Dawson, R.W.; Li, B.G. A GIS-Based Method of Lake Eutrophication Assessment. *Ecol. Model.* **2001**, *144*, 231–244. [[CrossRef](#)]
50. Luo, W.; Liu, C.C. Innovative Landslide Susceptibility Mapping Supported by Geomorphon and Geographical Detector Methods. *Landslides* **2018**, *15*, 465–474. [[CrossRef](#)]
51. Cui, J.; Zhu, M.; Liang, Y.; Qin, G.; Li, J.; Liu, Y. Land Use/Land Cover Change and Their Driving Factors in the Yellow River Basin of Shandong Province Based on Google Earth Engine from 2000 to 2020. *ISPRS Int. J. Geo-Inf.* **2022**, *11*, 163. [[CrossRef](#)]
52. Shi, P.J.; Zhao, Z.; Chen, Y.; Sun, H.H. Study on Environmental Impact Assessment in Land Use Planning of Ganzhou Borough Based on DPSIR Model. *Adv. Mater. Res.* **2012**, *518–523*, 1210–1220. [[CrossRef](#)]
53. Cao, F.X.; Qi, C.J.; Li, G.R.; Zhong, C.Y.; Tang, D.S.; Xu, Y.F.; Peng, C.H. Climate Change Effects on Southern Subtropical and Tropical Tree Species in Ganzhou City, China. *Br. J. Environ. Clim. Change* **2012**, *2*, 163–179. [[CrossRef](#)] [[PubMed](#)]

54. Wang, J.F.; Li, X.H.; Christakos, G.; Liao, Y.L.; Zhang, T.; Gu, X.; Zheng, X.Y. Geographical Detectors-Based Health Risk Assessment and Its Application in the Neural Tube Defects Study of the Heshun Region, China. *Int. J. Geogr. Inf. Sci.* **2010**, *24*, 107–127. [[CrossRef](#)]
55. Wang, J.F.; Xu, C.D. Geodetector: Principle and prospective. *ACTA Geogr. Sin.* **2017**, *72*, 116–134.
56. Wei, Y.J.; Wu, X.L.; Wang, J.G.; Yu, H.L.; Xia, J.W.; Deng, Y.S.; Zhang, Y.; Xiang, Y.; Cai, C.F.; Guo, Z.L. Identification of Geo-Environmental Factors on Benggang Susceptibility and Its Spatial Modelling Using Comparative Data-Driven Methods. *Soil Tillage Res.* **2021**, *208*, 104857. [[CrossRef](#)]
57. Yin, S.Q.; Nearing, M.A.; Borrelli, P.; Xue, X.C. Rainfall Erosivity: An Overview of Methodologies and Applications. *Vadose Zone J.* **2017**, *16*, 1–16. [[CrossRef](#)]
58. Liu, Y.; Zhao, W.W.; Liu, Y.X.; Pereira, P. Global Rainfall Erosivity Changes between 1980 and 2017 Based on an Erosivity Model Using Daily Precipitation Data. *Catena* **2020**, *194*, 104768. [[CrossRef](#)]
59. Wang, X.X.; Jia, K.; Liang, S.L.; Li, Q.Z.; Wei, X.Q.; Yao, Y.J.; Zhang, X.T.; Tu, Y.X. Estimating Fractional Vegetation Cover from Landsat-7 ETM+ Reflectance Data Based on a Coupled Radiative Transfer and Crop Growth Model. *IEEE Trans. Geosci. Remote Sens.* **2017**, *55*, 5539–5546. [[CrossRef](#)]
60. Xiao, Q.; Tao, J.P.; Xiao, Y.; Qian, F. Monitoring Vegetation Cover in Chongqing between 2001 and 2010 Using Remote Sensing Data. *Environ. Monit. Assess.* **2017**, *189*, 493. [[CrossRef](#)]
61. Yang, L.Q.; Jia, K.; Liang, S.L.; Wei, X.Q.; Yao, Y.J.; Zhang, X.T. A Robust Algorithm for Estimating Surface Fractional Vegetation Cover from Landsat Data. *Remote Sens.* **2017**, *9*, 857. [[CrossRef](#)]
62. Zhao, G.; Huang, Y.H.; Lin, J.S.; Jiang, F.S.; Ge, H.L.; Chen, P.J.; Li, X.G.; Zhan, Z.Z.; Zheng, Q.F. Effect of Discharge and Slope Gradient on Colluvial Deposits Erosion in Benggang. *Res. Soil Water Conserv.* **2014**, *2*, 11–16.
63. Chen, X.A.; Yang, J.; Xiong, Y.; Xiao, S.S. Research on the Soil Characteristics and Factors of Collapsing Erosion in the Red Soil Zone. *J. Hydraul. Eng.* **2013**, *44*, 1175–1181.
64. Liao, Y.S.; Tang, C.Y.; Yuan, Z.J.; Zhuo, M.N.; Huang, B.; Nie, X.D.; Xie, Z.Y.; Li, D.Q. Research Progress on Benggang Erosion and Its Prevention Measure in Red Soil Region of Southern China. *ACTA Pedol. Sin.* **2018**, *55*, 1297–1312.
65. Song, Y.J.; Liao, K.T.; Yang, J.; Zuo, J.C.; Xiao, L. Temporal and spatial variation of vegetation cover and its water and soil conservation driving in Tangbei River watershed. *J. Water Resour. Water Eng.* **2017**, *28*, 24–31.
66. Bennett, S.J.; Wells, R.R. Gully Erosion Processes, Disciplinary Fragmentation, and Technological Innovation. *Earth Surf. Process. Landf.* **2019**, *44*, 46–53. [[CrossRef](#)]
67. Zhao, F.F.; He, M.C.; Wang, Y.T.; Tao, Z.G.; Li, C. Eco-Geological Environment Quality Assessment Based on Multi-Source Data of the Mining City in Red Soil Hilly Region, China. *J. Mt. Sci.* **2022**, *19*, 253–275. [[CrossRef](#)]
68. Jiang, Z.Y.; Wang, X.D.; Zhang, S.Y.; He, B.; Zhao, X.L.; Kong, F.L.; Feng, D.; Zeng, Y.C. Response of Soil Water Dynamics to Rainfall on A Collapsing Gully Slope: Based on Continuous Multi-Depth Measurements. *Water* **2020**, *12*, 2272. [[CrossRef](#)]
69. Zhan, Q.; Wang, S.; Li, W.; Guo, F.; Yan, J. Analysis of Failure Models and Deformation Evolution Process of Geological Hazards in Ganzhou City, China. *Front. Earth Sci.* **2021**, *9*, 731447. [[CrossRef](#)]